JOURNAL OF APPLIED POLYMER SCIENCE VOL. 18, PP. 3137–3151 (1974)

Modified Bead Spring Theory of Dilute Polymer Solutions. III. Inclusion of Multiple Relaxation Times

A. E. EVERAGE, JR.,* and R. J. GORDON, *Department of Chemical Engineering, University of Florida, Gainesville, Florida 32611*

Synopsis

A previously derived constitutive equation, representing a blending of the molecular dumbbell theory and a continuum theory of anisotropic fluids, has been extended to the multidumbbell (Rouse-Zimm) case. The equation thus derived yields predictions equivalent to the Rouse-Zimm theory in small-amplitude dynamic shearing, with the exception that the introduction of an "effective molecular weight" as the concentration of polymer is increased is no longer required. In simple shearing flow, the theory predictions are far superior to those of the Rouse-Zimm model, yielding realistic non-Newtonian viscosity behavior, a positive primary normal stress difference, and a negative secondary normal stress difference. In stress relaxation following the cessation of steady shearing flow, the rate of relaxation is found to depend to the initial velocity gradient, but the effect is predicted to be too small to be observed experimentally in typical dilute polymer solutions. The effects of molecular weight, molecular weight distribution, and polymer–solvent interaction are explicitly accounted for, and in all cases the theory predictions are in excellent qualitative agreement with accepted experimental behavior.

INTRODUCTION

The theoretical development of constitutive equations for dilute polymer solutions has generally been approached from two distinct viewpoints: continuum mechanics or molecular theory. Each of these procedures suffers from certain disadvantages which detract from their utility. For example, the continuum theories invariably contain a large number of unknown constants which must be determined experimentally; and, in addition, the theories yield no information on the relationship between these constants and the molecular properties of the fluid under consideration. The molecular theories, on the other hand, must necessarily be based on rather idealized hydrodynamic models of the polymer molecule in solution, such as the bead spring model[1]; and frequently these models must be significantly generalized and complicated, e.g., through the inclusion of "internal viscosity," [2] in order to describe various nonlinear effects such as a shear-thinning viscosity function. Furthermore, these molecular theories are

* Present address: Monsanto Textile Company, Technical Center, Pensacola, Florida 32575.

often not expressible in the form of an explicit constitutive equation, that is, an explicit relation between the stress tensor and the velocity field.

In a series of recent papers,[3-6] we have developed a constitutive equation for dilute polymer solutions which represents a "blend" of both continuum mechanics and molecular theory and eliminates many of the objections to these two procedures discussed above. The theory explicitly accounts for molecular weight, molecular weight distribution, and polymer–solvent interaction and contains but a single phenomenologic constant, ϵ, which is restricted to the range[3]

$$0 \leq \epsilon < 1.0.$$

The predictions of the theory have been shown to qualitatively describe a large variety of experimental data for both dilute and moderately concentrated polymer solutions. However, in the case of small amplitude data, e.g., η' and G' versus ω, the theory was found to be satisfactory only in the low-frequency range,[5] where it yielded predictions very similar to those of the well-accepted Rouse-Zimm model. For higher frequencies, the theory predictions began to deviate both quantitatively and qualitatively from the Rouse-Zimm results. This inability to describe high-frequency dynamic data is a consequence of the single relaxation time used in the theory. Similar difficulties appear in the calculation of the stress relaxation rate following the cessation of steady shearing flow.[4] In this case, the rate was predicted to be independent of initial velocity gradient, in disagreement with available data on concentrated polymer solutions[7] (dilute solution data is unavailable); and again, this appears to be due to the presence of a single relaxation time. To more realistically describe the time-dependent behavior of dilute polymer solutions, the presence of multiple relaxation times must be included; and that is the objective of the present work. As will be seen, the inclusion of multiple relaxation times also greatly improves the ability of the theory to describe steady flow phenomena.

THEORETICAL DEVELOPMENT

The basis of our original single-relaxation time theory was the "continuum" structured fluid theory developed by Ericksen.[8] Combining the results of Ericksen's theory with the molecular dumbbell model lead to the following expression for the stress tensor[4]:

$$\boldsymbol{\tau} + \theta \frac{\tilde{D}\boldsymbol{\tau}}{Dt} = 2 \frac{N_A c}{M} kT\theta(1 - \epsilon)\mathbf{D} \tag{1}$$

where

$$\frac{\tilde{D}\boldsymbol{\tau}}{Dt} = \frac{\partial \boldsymbol{\tau}}{\partial t} + \mathbf{v}\cdot\nabla\boldsymbol{\tau} - \boldsymbol{\Omega}\cdot\boldsymbol{\tau} + \boldsymbol{\tau}\cdot\boldsymbol{\Omega} - (1 - \epsilon)\mathbf{D}\cdot\boldsymbol{\tau} - \boldsymbol{\tau}\cdot(1 - \epsilon)\mathbf{D}. \tag{2}$$

In these equations, θ is the relaxation time, N_A is Avogadro's number, c is the polymer concentration, M is the molecular weight, k is Boltzmann's constant, T is the temperature, $\mathbf{v}$ is the velocity, $\boldsymbol{\Omega}$ is the vorticity tensor $[= {}^1/_2(\nabla\mathbf{v} - \nabla\mathbf{v}^t)]$, and $\mathbf{D}$ is the rate of strain tensor $[= {}^1/_2(\nabla\mathbf{v} + \nabla\mathbf{v}^t)]$.

This result is identical to the corresponding result from the dumbbell model, except that the rate of strain tensor is multiplied throughout by the value $(1 - \epsilon)$. This single modification strikingly improves the predictions of the theory for steady shearing flow, without significantly affecting the dynamic behavior, where the dumbbell theory gives reasonably good predictions for low frequencies. Thus, the continuum theory of Ericksen suggests that the "effective" velocity gradient acting on an isolated macromolecule in solution is given by

$$\nabla \mathbf{v} - \epsilon \mathbf{D}. \tag{3}$$

In order to describe high-frequency dynamic data accurately, it is well known that the simple dumbbell model must be extended to a multibead spring or Rouse-Zimm-type model.[1] Such an extension still suffers from the same unrealistic simple shearing predictions as the single dumbbell formulation, however. Our findings suggest that the substitution $\mathbf{D} \rightarrow (1 - \epsilon)\mathbf{D}$ into the Rouse-Zimm theory should greatly improve steady shearing results without affecting the already excellent predictions for dynamic data.

A convenient formulation of the Rouse-Zimm theory has recently been developed by Lodge and Wu.[9] These authors expressed the theory, for an arbitrary degree of hydrodynamic interaction, in the form of an explicit constitutive equation as follows:

$$\boldsymbol{\tau}_j + \theta_j \frac{\tilde{D}\boldsymbol{\tau}_j}{Dt} = 2 \frac{N_A c}{M} kT\theta_j \mathbf{D} \tag{4}$$

where

$$\frac{\tilde{D}\boldsymbol{\tau}_j}{Dt} = \frac{\partial \boldsymbol{\tau}_j}{\partial t} + \mathbf{v}\cdot\nabla\boldsymbol{\tau}_j - \boldsymbol{\Omega}\cdot\boldsymbol{\tau}_j + \boldsymbol{\tau}_j\cdot\boldsymbol{\Omega} - \mathbf{D}\cdot\boldsymbol{\tau}_j - \boldsymbol{\tau}_j\cdot\mathbf{D} \tag{5}$$

$$\boldsymbol{\tau} = \sum_{j=1}^{N} \boldsymbol{\tau}_j \tag{6}*$$

N is the number of "submolecules" in a chain, and θ_j, the jth relaxation time, is given by

$$\theta_j = \frac{\theta_1 \lambda_1}{\lambda_j} \tag{7}$$

where the λ_j's are characteristic values of the matrix

$$B_{i,k} = H_{i,k} - H_{i-1,k} - H_{i,k-1} + H_{i-1,k-1} \tag{8}$$

and the $H_{i,k}$'s are defined by

$$H_{i,i} = 1$$

$$H_{i,j} = h/|i - j|^{1/2} \tag{9}$$

$$h = \zeta(6\pi^3)^{-1/2}(\eta_S b)^{-1}. \tag{10}$$

*Note that $\tau_j = \mathbf{P}_j^* - n_0 kT\boldsymbol{\delta}$, where $\mathbf{P}_j^*$ is the jth contribution to the stress tensor as given by Lodge and Wu, and n_0 is the number of macromolecules per unit volume.

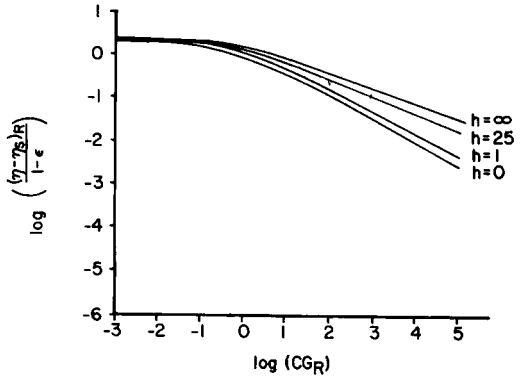

Fig. 1. Effect of hydrodynamic interaction on viscosity–shear rate relation.

Here, ζ is the bead friction coefficient, η_S is the solvent viscosity, b is the r.m.s. length of a "submolecule" at rest, and h is a measure of the "strength" of bead–bead hydrodynamic interaction. By making the substitution $\mathbf{D} \rightarrow (1 - \epsilon)\mathbf{D}$ in eqs. (4) and (5), we arrive at what might aptly be called a *continuum-modified multibead spring theory.*

THEORY PREDICTIONS

Effects of Hydrodynamic Interaction

The effects of hydrodynamic interaction on the predictions of the continuum-modified multibead spring model may be determined by calculating material functions for various values of the parameter h. It is interesting to note, however, that h does not appear explicitly in the constitutive equation and therefore does not affect the form of the model expressions for any material function. Parameter h appears only in the matrix $H_{i,j}$ and as a result affects only the calculation of the relaxation times θ_j.[9]

Small-Amplitude Oscillatory Shear Flow

For the case of small amplitude, oscillatory shearing flow, eqs. (4) → (7), with $\mathbf{D}$ replaced by $(1 - \epsilon)\mathbf{D}$, lead to the following expressions for the storage and loss moduli:

$$G_R' = \frac{G'}{cRT} M_e = \sum_{j=1}^{N} \frac{\omega_R^2(\theta_j/\theta_1)^2}{1 + \omega_R^2(\theta_j/\theta_1)^2} \tag{11}$$

$$G_R'' = \frac{G'' - \omega\eta_S}{cRT} M_e = \sum_{j=1}^{N} \frac{\omega_R(\theta_j/\theta_1)}{1 + \omega_R^2(\theta_j/\theta_1)^2} \tag{12}$$

where $\omega_R = \theta_1\omega$, R is the gas law constant, and $M_e = M/(1 - \epsilon)$. These expressions are identical with the corresponding results in the multibead spring model, except that in the latter case, $M_e = M$.[1] For very dilute solutions or very low molecular weights, where the degree of non-Newtonian behavior is slight, ϵ is small and $M_e \approx M$. On the other hand, as the solu-

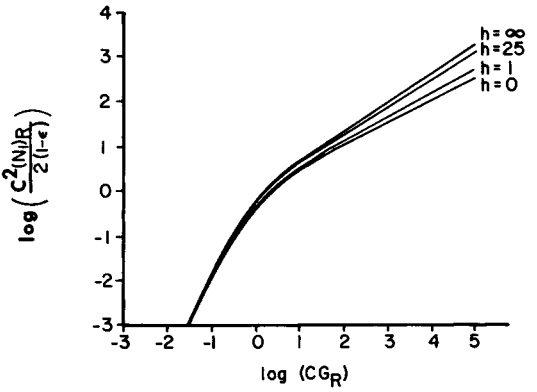

Fig. 2. Effect of hydrodynamic interaction on primary normal stress difference–shear rate relation.

tion concentration is raised, ϵ increases and $M_e > M$. Ferry and co-workers have observed precisely this behavior experimentally.[1,10] That is, in the comparison of the Rouse-Zimm theory with experimental dynamic data, it was necessary to allow M to be an adjustable parameter for the more concentrated solutions, with the value of "$M_{\text{effective}}$" increasing with concentration.[10] For very dilute solutions, $M_{\text{effective}}$ was found to be equal to the true polymer molecular weight. The present theory thus eliminates this additional difficulty associated with the multibead spring model as well as providing realistic predictions of non-Newtonian behavior.

Simple Shearing Flow

For simple shearing flow ($v_1 = Gx_2$, $v_2 = 0$, $v_3 = 0$), the continuum-modified multibead spring theory yields the following expressions for the non-Newtonian viscosity and primary normal stress difference:

$$(\eta - \eta_S)_R = \frac{\eta - \eta_S}{n_0 kT\theta_1} = (1 - \epsilon) \sum_{j=1}^{N} \frac{\theta_j/\theta_1}{1 + (CG_R\theta_j/\theta_1)^2} \tag{13}$$

$$(N_1)_R = \frac{\tau_{11} - \tau_{22}}{n_0 kT} = 2(1 - \epsilon) \sum_{j=1}^{N} \frac{G_R{}^2(\theta_j/\theta_1)^2}{1 + (CG_R\theta_j/\theta_1)^2} \tag{14}$$

where $G_R = \theta_1 G$, $C^2 = \epsilon(2 - \epsilon)$, and n_0 is the number of macromolecules per unit volume ($N_A c/M$). A comparison of these expressions with those for the reduced dynamic moduli G_R' and G_R'' in the Rouse-Zimm theory[1] shows that the dependence of the quantity $(\eta - \eta_S)_R/(1 - \epsilon)$ on CG_R is identical to the dependence of $(G'' - \omega\eta_S)_R/\omega_R$ on ω_R in the Rouse-Zimm theory. Similarly, $C^2(N_1)_R/2(1 - \epsilon)$ turns out to have the same functional dependence on CG_R as does G_R' on ω_R in the Rouse-Zimm theory. As a result of this, the predicted effects of variations in hydrodynamic interaction on the non-Newtonian viscosity and primary normal stress difference in the present theory may be obtained from calculations done previously for the Rouse-Zimm theory. For example, Figures 1 and 2 have been constructed using the tabulated values of G_R' and G_R'' in Ferry.[1]

The viscosity predictions in Figure 1 are typical of those obtained experimentally for dilute polymer solutions. This is in marked contrast to the Rouse-Zimm theory, which predicts no shear rate dependence at all for η. The figure indicates that the primary effect of increasing hydrodynamic interaction is a gradual increase of the slope in the high shear rate region from a value of $-1/2$ for the free draining model ($h = 0$), to $-1/3$ for the case of dominant hydrodynamic interaction ($h = \infty$). In the case of the primary normal stress difference, Figure 2, increasing values of h result in a similar increase in the slope in the high shear rate region. At low shear rates, N_1 is proportional to G^2, while for increasing values G of a proportionality of the form N_1 oc G^β, $\beta < 2$ is observed. This behavior is again typical of that seen with polymer solutions, although few measurements have been reported at truly "dilute" concentration levels. Note that the Rouse-Zimm theory predicts $N_1 \sim G^2$ for all values of G[11].

The secondary normal stress difference may also be calculated with ease in the present theory and is found to be

$$(N_2)_R = \frac{\tau_{22} - \tau_{33}}{n_0 kT} = -\epsilon(1 - \epsilon) \sum_{j=1}^{N} \frac{G_R^2(\theta_j/\theta_1)^2}{1 + (CG_R\,\theta_j/\theta_1)^2}. \tag{15}$$

From eqs. (14) and (15), we have

$$\frac{N_2}{N_1} = \frac{-\epsilon}{2}$$

and since ϵ is usually quite small, N_2 is predicted to be a small negative quantity, again in agreement with the generally accepted rheological behavior of polymer solutions.[12-15] The Rouse-Zimm theory, on the other hand, predicts $N_2 = 0$ (recall that the present results reduce to those of the Rouse-Zimm theory for $\epsilon = 0$).

Bird-Carreau Relation for Relaxation Times

The unknown parameters h and ϵ in the present theory are determined by comparing the predicted solution behavior with experimental results. The parameter h, however, is rather difficult to use, since its value cannot be obtained directly from experimental data for any material function. Rather, a series of theoretically calculated curves for various values of h must be visually compared with the data to determine the specific value of h giving the best fit. This method requires experimental data over a broad range of shear rates or frequencies and is not well suited for computer analysis.

As discussed above, variations in hydrodynamic interaction affect only the calculation of the relaxation times, θ_i. The results in Figures 1 and 2 indicate that increasing values of h produce a smooth transition from the free draining coil ($h = 0$), for which

$$\theta_j \cong \frac{\theta_1}{j^2} \tag{16}$$

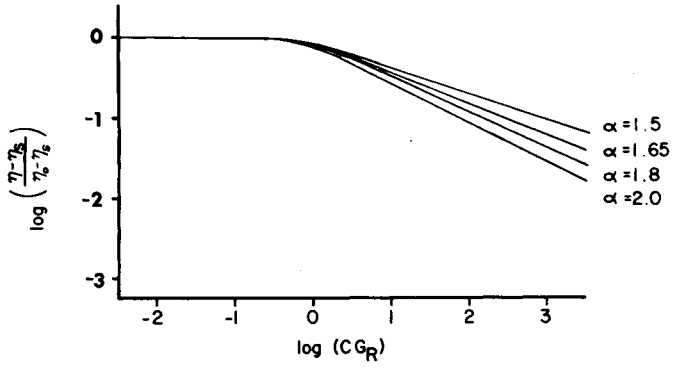

Fig. 3. Effect of Bird-Carreau[18] parameter α on viscosity–shear rate relation. Note that effects are analogous to those obtained by varying hydrodynamic interaction.

to the case of dominant hydrodynamic interaction ($h = \infty$), where

$$\theta_j = \frac{\theta_j}{j^{1.5}} \qquad j > 7. \tag{17}$$

Such considerations suggest that an empirical relation of the form

$$\theta_j = \frac{\theta_1}{j^{\alpha}} \tag{18}$$

should be useful as an alternative to the lengthy computations required for intermediate values of h. This relationship was used by Spriggs in a constitutive theory similar in form to that presented here.[16] We have found eq. (18) to lead to rather unrealistic predictions of η for large values of α (which are required to describe highly non-Newtonian systems). Bird and Carreau were also led to similar conclusions,[17] and the more recent Bird-Carreau model utilizes a relationship between the relaxation times of the form[18]

$$\theta_j = \frac{\theta_1}{(1 + j)/(2)^{\alpha}}. \tag{19}$$

This expression leads to much more realistic predictions of material response.

The inclusion of an explicit expression for θ_j of the form of eq. (19) in the present theory results in a predicted material dependence on the parameter α that is essentially identical to the behavior illustrated in Figures 1 and 2 for variations in h. Figure 3 illustrates the effects of variations in α on the non-Newtonian viscosity. Here we have plotted $\eta - \eta_S/(\eta_0 - \eta_S)$ versus CG_R, where η_0 is the zero-shear viscosity. Clearly, changes in α affect primarily the slope in the high shear rate region of the curves, in a manner quite similar to variations in h. However, the parameter α, in contrast to h, is simply related to the experimentally observed slope, S, in the high shear rate region of the viscosity curve by the relation

$$S = \frac{1 - \alpha}{\alpha} \tag{20}$$

(an identical result holds for the Bird-Carreau theory). As a consequence, the determination of α in any particular application is generally a simple procedure. Furthermore, utilizing eq. (19) in the present theory results in a constitutive equation that can be modified to include polydispersity in a straightforward manner. The classical hydrodynamic interaction formulation, although theoretically more appealing, presents a very formidable computational task in this regard.

Polydispersity Correction

In the case of dilute polydisperse solutions, the previous constitutive equation is assumed to apply to each molecular weight fraction, the total stress being obtained by a summation over all fractions. The present theory then takes the form

$$\tau_j^i + \theta_j^i \frac{\tilde{D}\tau_j^i}{Dt} = 2\frac{N_A c_i}{M_i} kT\theta_j^i(1-\epsilon)\mathbf{D} \qquad j = 1, \ldots, N_i \tag{21}$$

$$\mathbf{S} = -p\boldsymbol{\delta} + 2\eta_S\mathbf{D} + \sum_i \sum_{j=1}^{Ni} \tau_j^i \tag{22}$$

where i refers to a particular molecular weight species and N_i is the number of "submolecules" for that species. The relaxation times θ_j^i are obtained from the relation

$$\theta_j^i = \frac{\eta_S[\eta]_{0i}M_i}{(z(\alpha)-1)NakT(1-\epsilon)(1+j)^\alpha} = \frac{\eta_S K M_i^{1+a}}{(z(\alpha)-1)NakT(1-\epsilon)(1+j)^\alpha} \tag{23}$$

where $[\eta]_{0i}$ is the zero shear rate intrinsic viscosity of a monodisperse solution corresponding to molecular weight M_i, K and a are the Mark-Houwink constants (assumed independent of molecular weight), and $z(\alpha)$ is the Riemann Zeta function,[19]

$$z(\alpha) = \sum_{s=1}^{\infty} \frac{1}{s^\alpha}.$$

We next assume that the molecular weight distribution may be suitably represented by the Schulz-Zimm distribution[20,21]

$$dn = \left(\frac{z+2}{M_w}\right)^{z+1}\left(\frac{M^z}{z!}\right)\exp\left\{\frac{-(z+2)}{M_w}M\right\}dM \tag{24}$$

where dn is the fraction of macromolecules with molecular weights in the range M to $M + dM$, and z is defined by

$$\frac{z+2}{z+1} = \frac{M_w}{M_n}. \tag{25}$$

The parameter z characterizes the breadth of the molecular weight distribution and may range from -1 to ∞, corresponding to $M_w/M_n = \infty$

and $M_w/M_n = 1.0$, respectively. The commonly observed most probable distribution corresponds to $z = 0$, and $z = 1$ characterizes the case of vinyl polymerization terminated by free-radical recombination.

EXPLICIT MODEL PREDICTIONS USING EQ. (19)

The expressions developed so far account for the effects of polydispersity (through the parameter z), polymer–solvent interaction (through the Mark-Houwink constants K and a), and temperature (assuming ϵ and α are independent of temperature and that the temperature dependence of η_S, K, and a is known or can be estimated). Thus, we have at our disposal an explicit constitutive equation, which yields realistic predictions for steady shearing flow, accounts for the effects of a variety of physicochemical variables, and contains only two arbitrary constants, α and ϵ. In the following discussion, we examine the ability of this constitutive equation to describe a variety of intrinsic viscosity shear rate data, both for monodisperse and polydisperse solutions, with differing degrees of solvent power. Since it is assumed in the theory that the solution is so dilute that intermolecular interactions may be neglected, intrinsic viscosity data, where the specific viscosity is extrapolated to zero concentration, form an ideal basis with which to test these results.

The theoretical predictions for the intrinsic viscosity are found to be as follows:

Monodisperse solutions:

$$\frac{[\eta]}{[\eta]_0} = \frac{1}{z(\alpha) - 1} \sum_{j=2}^{N} \frac{j^\alpha}{j^{2\alpha} + (B\beta/(z(\alpha) - 1))^2} \tag{26}$$

Polydisperse solutions:

$$\frac{[\eta]}{[\eta]_0} = \frac{(z + 2)^{z+2+a}}{(z(\alpha) - 1)\Gamma(z + 2 + a)} \int_0^\infty x^{z+1+a} \exp\{-(z + 2)x\} \times \sum_{j=2}^{N} \frac{j^\alpha}{j^{2\alpha} + (B\beta_w x^{1+a}/(z(\alpha) - 1))^2} dx \tag{27}$$

$$[\eta]_0 = \frac{KM_w{}^a\Gamma(z + 2 + a)}{(z + 2)^a\Gamma(z + 2)}. \tag{28}$$

In these expressions, $B^2 = \epsilon(2 - \epsilon)/(1 - \epsilon)^2$, Γ is the gamma function, and β and β_w are dimensionless shear rates defined by

$$\beta = \frac{\eta_S K M^{1+a} G}{N_A k T} \tag{29}$$

$$\beta_w = \frac{\eta_S K M_w{}^{1+a} G}{N_A k T}. \tag{30}$$

The behavior of eq. (27) is plotted in Figures 4 and 5. Figure 4 illustrated the effects of polydispersity. These results have been obtained as-

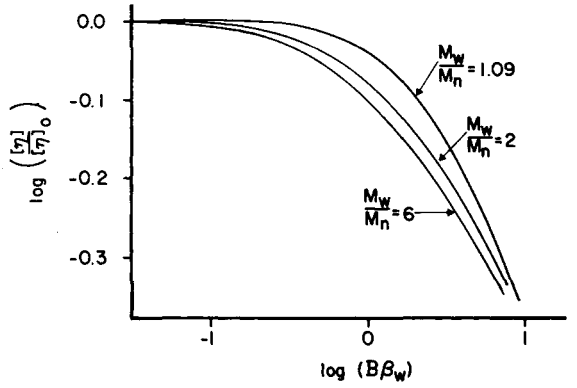

Fig. 4. Model predictions: effect of polydispersity on intrinsic viscosity–shear rate relation.

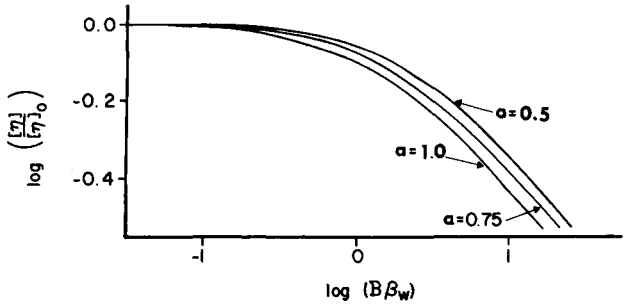

Fig. 5. Model predictions: effect of polymer–solvent interaction (as reflected by Mark-Houwink exponent a) on viscosity–shear rate relation.

suming the typical values $a = 0.75$, $\alpha = 2.0$, and the specified values of M_w/M_n. The curves indicate that the more polydisperse solutions show an earlier deviation from Newtonian behavior, with a smaller slope in the high shear region. These are the general effects observed experimentally.[22,23]

Figure 5 illustrates the predicted effect of the Mark-Houwink-Sakurada exponent a on the $[\eta]/[\eta]_0$-versus-β_w relationship. In the calculation of these results, the values $\alpha = 2.0$ and $z = 0$ have been used. The parameter a is a measure of polymer–solvent interaction, with the value $a = 0.5$ corresponding to a theta solvent. Larger values of a correspond to increasingly better solvents. The results in Figure 5 show that the better solvents show earlier departure from Newtonian behavior, again in agreement with accepted experimental trends.[24–26]

We now turn to some specific intrinsic viscosity–shear rate data. Suzuki, Kotaka, and Inagaki[24] have investigated the effects of molecular weight and polymer–solvent interaction on the intrinsic viscosity–β_w relation. Their experimental results for four solutions are plotted in Figures 6 and 7. Figure 6 illustrates the effect of polymer–solvent interaction for solutions of polystyrene ($M_w = 6.0 \times 10^6$, $M_w/M_n = 1.2$) in benzene and Aroclor (a chlorinated diphenyl). The polymer–solvent interaction, or solvent power,

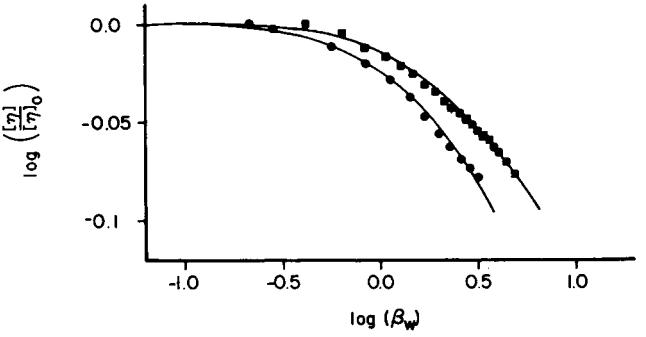

Fig. 6. Log[η]/[η]$_0$ vs. log β_w for polystyrene in benzene(●) and Aroclor (■)[24]: (—) model predictions for polydisperse solutions.

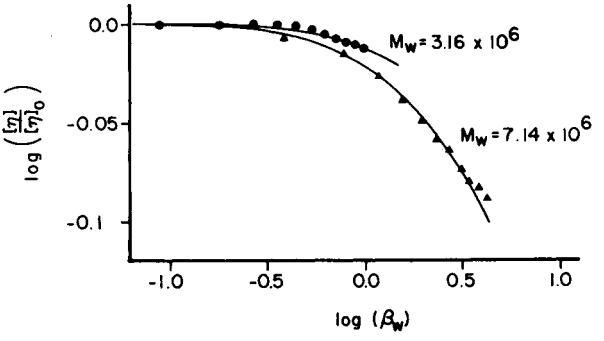

Fig. 7. Log [η]/[η]$_0$ vs. log β_w for polystyrene in benzene[24]: (—) model predictions for polydisperse solution.

is characterized by the hydrodynamic expansion factor $[[\eta]_0/[\eta]_{0,\theta}]^{1/3}$, where $[\eta]_{0,\theta}$ is the zero-shear rate intrinsic viscosity in a theta solvent. These values are 1.80 and 1.31 for polystyrene in benzene and Aroclor, respectively. The predictions of eq. (27), using the literature values of a (0.77 for benzene[27] and 0.64 for Aroclor[28]) are represented by the solid lines in the figure, and the corresponding values of ϵ and α are tabulated in Table I.

Figure 7 illustrates the effect of weight-average molecular weight on the intrinsic viscosity–β_w relation, for two polystyrene fractions ($M_w = 3.16 \times 10^6$, $M_w = 7.14 \times 10^6$) in benzene. Although the M_w/M_n values for the fractions were not given we used the same value (1.2) reported by Suzuki et al.[24] for the solvent study above. The resulting theory predictions are represented by the solid lines, and the corresponding values of α and ϵ are tabulated in Table I. For both Figures 6 and 7, the theoretical curves were obtained as follows: For given values of a and z, curves of $[\eta]/[\eta]_0$ versus $B\beta_w$ for different values of α were calculated from eq. (27). These curves were shifted along the log β_w axis so as to obtain superposition with the experimental data, and the value of α giving the best fit thereby obtained. The value of B and thus ϵ was then calculated from the extent of the horizontal shift.

TABLE I
Summary of Intrinsic Viscosity–Shear Rate Data

Polymer	Solvent	Temp., °C	M_w	α	$[\eta]_0$, dl/g	ϵ
Polystyrene	benzene	30	6.0×10^6	1.28	11.65	0.73
	Aroclor	40	6.0×10^6	1.20	4.50	0.77
	benzene	30	3.16×10^6	1.28	7.04	0.57
	benzene	30	7.14×10^6	1.28	13.5	0.71
Cellulose nitrate	ethyl acetate	25	0.37×10^6	1.70	10.1	0.35
	ethyl acetate	25	1.9×10^6	1.70	41.3	0.10
	ethyl acetate	25	5.5×10^6	1.70	104	0.032
Sodium car-	water	25	9.1×10^5	4.40	1370	3.4×10^{-4}
boxymethyl-	0.01M NACl	25	9.1×10^5	1.57	46.6	0.48
cellulose	0.2M NACl	25	9.1×10^5	1.47	20.7	0.75

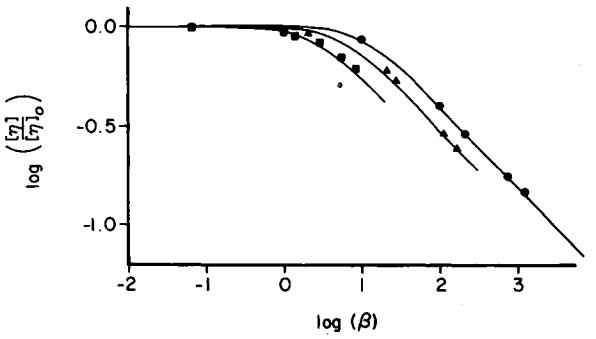

Fig. 8. Log $[\eta]/[\eta]_0$ vs. log β for solutions of cellulose nitrate in ethyl acetate[29]: (●) $M_w = 5.5 \times 10^6$; (▲) $M_w = 1.9 \times 10^6$; (■) $M_w = 0.36 \times 10^6$; (—) model predictions for monodisperse solution.

Lohmander and Svensson[29] have also studied the effects of molecular weight on the $[\eta]/[\eta]_0$-versus-β_w relation for various fractions of cellulose nitrate in ethyl acetate. Their results for $M_w = 5.5 \times 10^6$, 1.9×10^6, and 0.36×10^6 are plotted in Figure 8. The distribution widths for these fractions were not reported, thus precluding the application of eq. (27). However, in order to gain some insight into the molecular weight dependence of ϵ, the predictions of eq. (26) for monodisperse solutions have been compared to these data. The monodisperse model predictions are indicated by the solid lines in the Figure, and the calculated values of α and ϵ are tabulated in Table I. It is clear that the theory is capable of quite accurately describing this data.

Figure 9 illustrates the intrinsic viscosity–shear rate relation for a polyelectrolyte (sodium carboxymethylcellulose) at different ionic strengths, as reported by Lohmander and Stromberg.[30] Here again, the solutions were assumed to be monodisperse, and α and ϵ were calculated from eq. (26). The values thus obtained are also listed in Table I. In Figures 8 and 9, the theoretical curves were calculated as follows: The slopes in the high shear

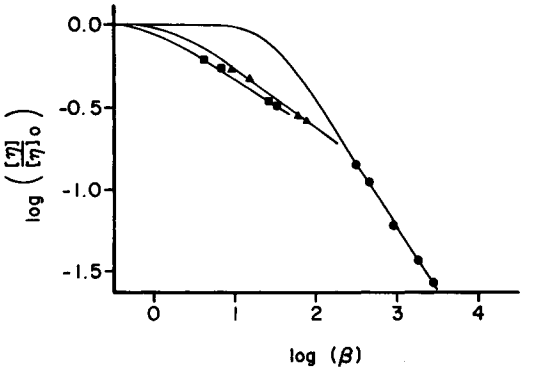

Fig. 9. Log $[\eta]/[\eta]_0$ vs. log β for solutions of sodium carboxymethylcellulose in aqueous NACl solutions[30]: (●) NACl molarity = 0.0; (▲) NACl molarity = 0.01; (■) NACl molarity = 0.2; (—) model predictions for monodisperse solutions.

rate region was measured, and from eq. (20) α was calculated. A plot of $[\eta]/[\eta]_0$ versus $B\beta$ was then made using eq. (26) and superimposed with the experimental data; the measured shift then yielded B.

Figures 6–9 illustrate the ability of the current model to accurately describe a wide variety of experimental intrinsic viscosity–shear rate data. In each figure, the data have been fit using only the two adjustable parameters α and ϵ. The value of α varies between 1.20 and 1.70 for all the solutions, except the sodium carboxymethylcellulose (CMC) in water. In water, CMC is highly extended, due to the mutual repulsion of adjacent carboxyl groups. Thus, we can anticipate rather abnormal viscosity behavior as compared to the nonelectrolyte solutions. The values of ϵ range from 3.35×10^{-4} up to 0.766, reflecting primarily the large range of β (or β_w) over which non-Newtonian effects first appear. The dependence of ϵ on molecular weight and solvent power appears to be rather obscure at present.

Stress Relaxation

As we noted earlier, our single relaxation time-modified bead spring theory lead to the prediction that the rate of stress relaxation following the cessation of simple shearing flow was independent of initial velocity gradient G. In the present theory, stress relaxation following steady shearing flow is described by

$$\frac{\tau_{ij}(t)}{\tau_{ij}(0)} = \frac{\sum_{j=2}^{\infty} \frac{j^\alpha \exp\left(-tj^\alpha/\theta_1 2^\alpha\right)}{j^{2\alpha} + (2^\alpha C\,\theta_1 G)^2}}{\sum_{j=2}^{\infty} \frac{j^\alpha}{j^{2\alpha} + (2^\alpha C\theta_1 G)^2}} \tag{31}$$

where $C^2 = \epsilon(2 - \epsilon)$ and t is the time following the cessation of flow. Using the typical values $\eta_S = 0.01$ poise, $\alpha = 2.0$, $\epsilon = 0.1$, $[\eta]_0 = 10.0$ dl/g, $M = 10^6$, and $T = 298°$K, we find

$$\theta_1 = 1.74 \times 10^{-4} \text{ sec.}$$

TABLE II
Stress Relaxation Predictions—Monodisperse Solutions

Time, sec	$\tau_{ij}(t)/\tau_{ij}(0)$		
	G = 100 sec^{-1}	G = 1000 sec^{-1}	G = 10,000 sec^{-1}
	a. $\theta = 1.74 \times 10^{-4}$ sec		
1.0×10^{-7}	0.97	0.97	0.96
1.0×10^{-6}	0.90	0.90	0.88
1.0×10^{-5}	0.70	0.70	0.66
1.0×10^{-4}	0.28	0.28	0.23
1.0×10^{-3}	0.001	0.001	0.001
1.0×10^{-2}	0.000	0.000	0.000
	b. $\theta = 1.74 \times 10^{-3}$ sec		
1.0×10^{-7}	0.99	0.99	0.97
1.0×10^{-6}	0.97	0.96	0.90
1.0×10^{-5}	0.90	0.88	0.71
1.0×10^{-4}	0.70	0.66	0.32
1.0×10^{-3}	0.28	0.23	0.034
1.0×10^{-2}	0.001	0.001	0.000

The corresponding values of $\tau_{ij}(t)/\tau_{ij}(0)$ are listed in Table II versus t, for various values of G. Although the rate of relaxation does increase with increasing G, the effect is extremely small. It was suspected that this was due to the rather small value of the principle relaxation time. (Relaxation times for concentrated polymer solutions and melts, where the effect of G on relaxation rate is pronounced, are 2 to 4 orders of magnitude larger.) To test this hypothesis, we recalculated $\tau_{ij}(t)/\tau_{ij}(0)$ using a value of $\theta_1 = 1.74 \times 10^{-3}$ sec. As indicated in Table II, the effect of increasing G is much more pronounced.

SUMMARY

A continuum-modified multibead spring theory has been developed, which includes the Rouse-Zimm theory as a special case ($\epsilon = 0$). The theory yields realistic predictions for steady shearing flow, including a non-Newtonian viscosity function, a nonzero positive N_1, and a nonzero negative N_2, while at the same time the dynamic viscosity predictions are similar to those of the Rouse-Zimm theory. The effects of molecular weight, molecular weight distribution, and polymer solvent interaction are explicitly accounted for. The theory was found to quantitatively describe a variety of intrinsic viscosity–shear rate data.

Acknowledgment is made to the National Science Foundation under Grant GK-31590 for partial support of this research.

References

1. J. D. Ferry, *Viscoelastic Properties of Polymers*, 2nd ed., Wiley, New York, 1970.
2. A. Peterlin, in *Advances in Macromolecular Chemistry*, Vol. 1, Academic Press, New York, 1968, W. M. Pasika, Ed., p. 225.
3. R. J. Gordon and W. R. Schowalter, *Trans. Soc. Rheol.*, **16**, 79 (1972).
4. R. J. Gordon and A. E. Everage, Jr., *J. Appl. Polym. Sci.*, **15**, 1903 (1971).
5. A. E. Everage, Jr., and R. J. Gordon, *J. Appl. Polym. Sci.*, **16**, 1967 (1972).
6. A. E. Everage, Jr., and R. J. Gordon, *Amer. Inst. Chem. Eng. J.*, **17**, 1257 (1971).
7. P. J. Carreau, I. F. Macdonald, and R. B. Bird, *Chem. Eng. Sci.*, **23**, 901 (1968).
8. J. L. Ericksen, *Kolloid Z.*, **173**, 117 (1960).
9. A. S. Lodge and Y. Wu, *Rheol. Acta*, **10**, 539 (1971).
10. J. E. Frederick, N. W. Tschoegl, and J. D. Ferry, *J. Phys. Chem.*, **68**, 1974 (1964).
11. M. C. Williams, *J. Chem. Phys.*, **42**, 2988 (1965); *ibid.*, **43**, 4542 (1965).
12. R. I. Tanner, *Trans. Soc. Rheol.*, **14**, 483 (1970).
13. M. J. Miller and E. B. Christiansen, *Amer. Inst. Chem. Eng. J.*, **18**, 600 (1972).
14. R. F. Ginn and A. B. Metzner, *Trans. Soc. Rheol.*, **13**, 429 (1969).
15. O. Olabisi and M. C. Williams, *Trans. Soc. Rheol.*, **16**, 727 (1972).
16. T. W. Spriggs, *Chem. Eng. Sci.*, **20**, 931 (1965).
17. R. B. Bird, personal communication.
18. R. B. Bird and P. J. Carreau, *Chem. Eng. Sci.*, **23**, 427 (1968).
19. M. Abramowitz and I. A. Segun, *Handbook of Mathematical Functions*, Dover Publications, New York, 1965.
20. B. H. Zimm, *J. Chem. Phys.*, **16**, 1099 (1948).
21. L. H. Peebles, Jr., *Molecular Weight Distributions in Polymers*, Interscience, New York, 1971.
22. W. W. Graessley and L. Segal, *Amer. Inst. Chem. Eng. J.*, **16**, 261 (1970).
23. R. L. Ballman and R. H. M. Simon, *J. Polym. Sci.*, **2**, 3557 (1964).
24. H. Suzuki, T. Kotaka, and H. Inagaki, *J. Chem. Phys.*, **51**, 1279 (1969).
25. G. C. Berry and E. F. Casassa, *J. Polym. Sci.*, **D4**, 1 (1970).
26. J. A. Subirana, *J. Chem. Phys.*, **41**, 3852 (1964).
27. J. Brandrup and E. H. Immergut, Eds., *Polymer Handbook*, Interscience, New York, 1967.
28. L. A. Holmes and J. D. Ferry, *J. Polym. Sci.*, **C23**, 291 (1968).
29. U. Lohmander and A. Svensson, *Makromol. Chem.*, **65**, 202 (1963).
30. U. Lohmander and R. Stromberg, *Makromol. Chem.*, **72**, 143 (1964).

Received April 9, 1974
Revised May 31, 1974